Cancer Biol Med 2025. doi: 10.20892/j.issn.2095-3941.2024.0540

ORGINAL ARTICLE

MDM1 overexpression promotes p53 expression and cell apoptosis to enhance therapeutic sensitivity to chemoradiotherapy in patients with colorectal cancer

Ningxin Ren[1]*, Hongxia Chen[1]*, Ying Huang[1,2], Jing Jin[3,4], Shaosen Zhang[1], Ruoqing Yan[1], Mengjie Li[1], Linlin Zheng[1], Shuangmei Zou[5], Yexiong Li[3], Wen Tan[1], Dongxin Lin[1,6]

[1]State Key Laboratory of Molecular Oncology, Department of Etiology and Carcinogenesis, Beijing Key Laboratory for Carcinogenesis and Cancer Prevention, National Cancer Center/National Clinical Research Center for Cancer/Cancer Hospital, Chinese Academy of Medical Sciences and Peking Union Medical College, Beijing 100021, China; [2]Department of Thoracic Surgery and Oncology, the First Affiliated Hospital of Guangzhou Medical University, State Key Laboratory of Respiratory Disease & National Clinical Research Center for Respiratory Disease, Guangzhou 510120, China; [3]Department of Radiation Oncology, National Cancer Center/National Clinical Research Center for Cancer/Cancer Hospital, Chinese Academy of Medical Sciences and Peking Union Medical College, Beijing 100021, China; [4]Department of Radiation Oncology, National Cancer Center/National Clinical Research Center for Cancer/Cancer Hospital & Shenzhen Hospital, Chinese Academy of Medical Sciences and Peking Union Medical College, Shenzhen 518100, China; [5]Department of Pathology, National Cancer Center/National Clinical Research Center for Cancer/Cancer Hospital, Chinese Academy of Medical Sciences and Peking Union Medical College, Beijing 100021, China; [6]Sun Yat-sen University Cancer Center, State Key Laboratory of Oncology in South China, Guangzhou 510060, China

ABSTRACT

Objective: Identifying biomarkers that predict the efficacy and prognosis of chemoradiotherapy is important for individualized clinical treatment. We previously reported that high murine double minute 1 (*MDM1*) expression in patients with rectal cancer is linked to a favorable chemoradiation response. In this study the role of MDM1 in the chemoradiotherapy response in colorectal cancer (CRC) patients was evaluated.

Methods: Colony formation and cell proliferation assays as well as xenograft models were used to determine if MDM1 expression affects the sensitivity of CRC cells to chemoradiation. RNA sequencing revealed that MDM1 regulates tumor protein 53 (*TP53*) expression and apoptosis. A series of molecular biology experiments were performed to determine how MDM1 affects p53 expression. The effects of inhibitors targeting apoptosis on MDM1 knockout cells were evaluated.

Results: Gene expression profiling revealed that MDM1 is a potential chemoradiotherapy sensitivity marker. The sensitivity of CRC cells to chemoradiation treatment decreased after MDM1 knockout and increased after MDM1 overexpression. MDM1 affected p53 expression, thereby regulating apoptosis. MDM1 overexpression limited YBX1 binding to *TP53* promoter, regulated *TP53* expression, and rendered CRC cells more sensitive to chemoradiation. In CRC cells with low MDM1 expression, a combination of apoptosis-inducing inhibitors and chemoradiation treatment restored sensitivity to cancer therapy.

Conclusions: The current study showed that MDM1 expression influences the sensitivity of CRC cells to chemoradiation by influencing p53 and apoptosis pathways, which is the basis for the underlying molecular mechanism, and serves as a possible predictive marker for chemoradiotherapy prognosis.

KEYWORDS Colorectal cancer; chemoradiotherapy sensitivity; MDM1; YBX1; TP53

Introduction

Capecitabine is frequently used in concurrent chemoradiotherapy for rectal cancer and can be converted to 5-fluorouracil (5-FU) upon absorption into the bloodstream[1]. Capecitabine exerts anti-tumor effects by inducing apoptosis and inhibiting cancer cell proliferation[2]. Radiotherapy also induces apoptosis in cancer cells[3]. One of the most challenging issues in cancer

*These authors contributed equally to this work.
Correspondence to: Wen Tan and Dongxin Lin
E-mail: tanwen@cicams.ac.cn and lindx@cicams.ac.cn
ORCID ID: https://orcid.org/0000-0002-7231-7838 and https://orcid.org/0000-0002-8723-8868
Received November 29, 2024; accepted January 21, 2025.
Available at www.cancerbiomed.org
©2025 The Authors. Creative Commons Attribution-NonCommercial 4.0 International License

treatment is treatment resistance, which is driven by complex factors, including DNA damage repair, cell cycle dysregulation, cell death, and mismatch repair deficiencies[4,5]. Resistance to chemoradiotherapy results in a poor treatment response, failure to prolong survival, and various side effects. Therefore, identifying markers that predict the efficacy and prognosis of chemoradiotherapy is crucial for clinical decision-making and patient survival. Many biomarkers have recently been studied as predictors of the response to concurrent chemoradiation therapy in locally advanced rectal cancer. However, the specificity and sensitivity of some research results have not reached the expected predictive value[6]. Therefore, further exploration is warranted.

Based on the urgent need to identify predictive markers of chemoradiotherapy efficacy as well as the issues in current marker research, we previously conducted an expression profile-related study to define differentially expressed genes (DEGs) that distinguish between good and poor responses to chemoradiotherapy[7]. The results of the experimental verification of the top 10 DEGs showed that *ZNF37A*, *ZNF121*, and *MDM1* ranked in the top 3 DEGs. Because studies on the mechanisms of action for *ZNF37A* and *ZNF121* have already been conducted, we planned to determine the specific mechanism by which murine double minute 1 (*MDM1*) expression affects chemoradiotherapy sensitivity. Both *MDM1* and murine double minute 2 (*MDM2*) were discovered in amplified extra chromosomal DNA sequences in the mouse 3T3DM cell line. Transcription factor p53 was characterized as a powerful tumor suppressor that inhibits tumor growth by promoting cell cycle arrest, apoptosis, and DNA repair[8-10]. E3 ubiquitin ligase MDM2 binds to p53 and induces p53 degradation, displaying carcinogenic activity[11]. The role of *MDM2* gene amplification in resistance to cancer treatment has been extensively studied[12]. Overexpression of *MDM2* can directly confer the resistance of tumor cells to cisplatin-induced apoptosis and also leads to cisplatin resistance by inducing p53 downregulation[13,14]. In contrast, research on MDM1, which does not exhibit tumorigenicity, remains limited[15]. *MDM1* encodes a nuclear protein that binds to and stabilizes microtubules and inhibits centriole duplication[16,17]. MDM1 maintains endoplasmic reticulum homeostasis through the spatial regulation of lipid droplet biosynthesis and links to intra-flagellar transport in photoreceptor cells[18,19]. To date, the correlation between MDM1 expression and chemoradiotherapy resistance has not been studied. Therefore, the purpose of the present study was as follows: (i) confirm the correlation between MDM1 and colorectal cancer (CRC) cell sensitivity to chemoradiotherapy; and (ii) demonstrate the specific mechanism by which MDM1 affects sensitivity to chemoradiotherapy through various experiments.

Materials and methods

Study participants and biospecimens

As described in our previous studies, the study group was comprised of 81 patients with locally advanced rectal cancer who were enrolled from January 2006 to June 2013 at the Cancer Hospital (Chinese Academy of Medical Sciences, Beijing, China)[7,20]. All of these participants underwent concurrent chemoradiotherapy preoperatively. The histologic tumor response to chemoradiotherapy was judged using the Mandard tumor regression grade (TRG). Briefly, 30 tissue samples of TRG1 (n = 7) and TRG2 (n = 23), 37 tissue samples of TRG3 (n = 37), and 14 tissue samples of TRG4 (n = 12) and TRG5 (n = 2) were grouped as responders, intermediate responders, and non-responders, respectively. The duration of disease-free survival (DFS) was recorded starting from the surgical intervention date to the time of tumor progression, death, or most recent follow-up evaluation. All 81 patients were tracked until 31 October 2021. None of the patients were lost to follow-up with a median follow-up time of 125 months. This study was approved by the Institutional Review Board of the Chinese Academy of Medical Sciences Cancer Institute (IRB no. 23/088–3827). The genome-wide expression profiling data of 81 patients with rectal cancer who received neoadjuvant chemoradiotherapy were submitted to the National Genomic Data Center database (https://ngdc.cncb.ac.cn/gsub/; project ID: PRJCA027384).

Cell lines and reagents

HT29 and HCT8 cells were grown in RPMI-1640 medium with 10% fetal bovine serum (FBS). RKO and HCT116 cells were grown in DMEM with 10% FBS. All cells were placed in a humidified incubator at 37°C in 5% CO_2. The chemotherapeutic drugs [5-FU (HY-90006) and oxaliplatin (HY-17371)] were acquired from MedChemExpress (Monmouth Junction, NJ, USA). Navitoclax/ABT-263 (A3007), birinapant/TL32711 (A4219), and idasanutlin/RG7388 (A3763) were obtained from APExBIO (Houston, TX, USA). All drugs were dissolved in dimethylsulfoxide [DMSO]

(Sigma-Aldrich, St. Louis, MO, USA) at appropriate concentrations and refrigerated at −80°C.

Establishment of CRC cell lines with MDM1 overexpression (OE) and knockout (KO)

Lentiviral particles containing the CRISPR/Cas9 system for stable MDM1-OE or MDM1-KO were procured from GeneChem (Shanghai, China). Stable MDM1 KO was accomplished using CRISPR to create single-guide RNA (sgRNA-1: 5′-CACCgCGAGTCTTGTAATTCCTCCG-3′, sgRNA-2: 5′-CACCgTCTGATCTAAGTCCAGCCCA-3′) sequences targeting the MDM1 genetic sequence. These sequences were subsequently inserted into the GV392 vector. HCT8 and RKO cells were transfected with the lentivirus, incubated in an incomplete medium for approximately 24 h, and subsequently selected with puromycin. Stable MDM1-OE and MDM1-KO cell lines were verified using western blotting and reverse transcription-quantitative polymerase chain reaction (RT-qPCR).

Cell viability and colony formation assays

Cells were seeded into 96-well (2,000 cells/well) and 6-well (2,000 cells/well) plates containing complete growth medium with or without chemotherapy (5 μg/mL of 5-FU and 1 μg/mL of oxaliplatin) and radiotherapy (2 Gy). Cell viability was tested daily using Cell Counting Kit-8 [CCK-8] (Dojindo Lab, Shanghai, China). CCK-8 reagents were incubated in each well at 37°C for 1.5 h and absorbance was detected at 450 nm. Cells were incubated with serial dilutions of 5-FU and oxaliplatin for determination of the half-maximal inhibitory concentration (IC_{50}) and CCK-8 absorbance was detected after 48 h. The IC_{50} values were obtained by non-linear regression analysis using GraphPad Prism software. Colonies were fixed in methanol and stained with 0.5% crystal violet after 1 week of cloning culture and the number was quantified using ImageJ software.

Extreme limiting dilution analysis

Cancer cells were seeded into 96-well plates at various cell densities (6.25, 12.5, 25, 50, 100, and 200 cells/well for RKO cells and 3, 6.25, 12.5, 25, 50, and 100 cells/well for HCT8 cells) with or without irradiation (2 Gy). After 1–2 weeks, the colony number was counted and a statistical analysis was performed online (http://bioinf.wehi.edu.au/software/elda/).

Quantitative real-time PCR analysis

Total RNA was isolated from the cell samples using an RNA-Quick Purification Kit (RN001; ES Science, Shanghai, China) and reverse-transcribed using PrimeScript RT Master Mix (RR0036A; TaKaRa, Dalian, China). The relative expression of the target genes was quantified *via* RT-qPCR using SYBR Green (RR820A; TaKaRa). **Table S1** presents the primer sets used for PCR amplification. Targeted gene mRNA levels were measured relative to GAPDH mRNA levels.

Western blot analysis

Cells were lysed using RIPA lysis buffer (P0013B; Beyotime, Shanghai, China) with the addition of phenylmethylsulfonyl fluoride [PMSF] (P0100; Solarbio, Beijing, China) and a phosphatase inhibitor cocktail (P003; NCM Biotech, Suzhou, China). After centrifugation at 12,000 rpm (16,000 × g) for 15 min, the protein supernatant concentration was measured using a BCA Protein Assay Kit (A53225; Thermo Fisher Scientific, Waltham, MA, USA). Next, 20 μg-protein samples were isolated on SDS-PAGE gels (MA0298; Meilunbio, Dalian, China) and transferred to PVDF membranes (Millipore, Billerica, MA, USA). Antibodies against GAPDH (60004-1-Ig), MDM1 (17575-1-AP), BAX (50599-2-Ig), non-POU domain-containing octamer-binding (NONO; 11058-1-AP), Y-box binding protein 1 (YBX1; 20039-1-AP), and p53 (10442-1-AP) were purchased from Proteintech (Rosemont, IL, USA). Splicing factor proline/glutamine-rich (SFPQ) protein antibody (ab177149) was purchased from Abcam (Cambridge, MA, USA). Antibodies against caspase-3 (#9662), cleaved caspase-3 (#9661), PARP (#9542), and cleaved PARP (#5625) were purchased from Cell Signaling Technology (Danvers, MA, USA). The signal was detected using an enhanced chemiluminescence western blotting substrate (Thermo Fisher Scientific) and visualized using an Amersham Imager 600. Quantification of the protein bands was performed by gray-scale scanning using ImageJ software.

Immunofluorescence flow cytometry

An annexin V/PI double-staining apoptosis detection kit (AD10; Dojindo Lab) was applied in this assay. Briefly, cells from the different treatment groups were digested and centrifuged at 1,000 rpm (111 × g) for 3 min. After two washes in PBS (MA00015; Meilunbio) the cells were subsequently incubated

with PI and annexin V reagents at room temperature for 15 min and detected by BD flow cytometry (LSRII; San Jose, CA, USA) within 1 h.

RNA sequencing analysis

Total RNA was extracted from MDM1-OE, MDM1-KO, and control cells in triplicate for sequencing (Novogene, Beijing, China). The RNA sequencing results were mapped to the human genome (Genome Research Consortium human build 38) by HISAT2. Significant differential expression was screened by referencing the *P* value and fold-change using the DESeq2 R package.

Proteomics analysis

Sequencing data (PTM BIO, Hangzhou, China) of protein samples from MDM1-OE and control HCT8 cells were retrieved using Proteome Discoverer (v2.4.1.15). Significantly differentially expressed proteins were selected at a P value < 0.05 and fold-change > 1.5 or < 0.67.

Immunoprecipitation assays

Cells were lysed in RIPA lysis buffer (P0013D; Beyotime) supplemented with PMSF (P0100; Solarbio) and phosphatase inhibitor cocktail (P003; NCM Biotech) for 1 h at 4°C. The supernatant was obtained after 15 min of centrifugation at 12,000 rpm (16,000 × g). Next, immunoprecipitation assays were conducted using the Dynabeads™ Protein G Immunoprecipitation Kit (10007D; Invitrogen, Carlsbad, CA, USA). Cell protein extracts and antibodies were incubated overnight with slow rotation at 4°C and eluted using an elution buffer. The obtained protein supernatant was isolated by SDS-PAGE for further western blotting and mass spectrometry analysis (PTM BIO). Antibodies for co-immunoprecipitation of rabbit immunoglobulin G (30000-0-AP), MDM1 (17575-1-AP), and YBX1 (20039-1-AP) were purchased from Proteintech.

Plasmids and small-interfering RNA transduction

Small-interfering RNAs (siRNAs) targeting YBX1 (5′-GGAGUUUGAUGUUGUUGAAGG-3′; control siRNA, 5′-UUCUCCGAACGUGUCACGUTT-3′) were purchased from Gene Pharma (Shanghai, China). Cells grown in 6-well plates were transfected with siRNAs using Lipofectamine 2000 (Invitrogen).

Dual-luciferase reporter assays

Dual-luciferase reporter assays were performed using the Nano-Glo Dual-Luciferase Reporter (NanoDLR™) system following the manufacturer's directions (N1620; Promega (Madison, WI, USA). CRC cells grown in 48-well plates (6×10^4 cells/well) were transfected with reporter plasmids using Lipofectamine 2000. After 1 day, Firefly and Renilla luciferase activities were measured using GENE5 software (BioTek, Winooski, Vermont, USA).

Chromatin immunoprecipitation (ChIP) assay

The SimpleChIP® Plus Sonication Chromatin IP Kit (#56383; Cell Signaling Technology) was used. Per the manufacturer's manual, 37% formaldehyde was added to the complete growth medium for a cross-linking reaction. The reaction was terminated with glycine (Sigma-Aldrich) after 10 min. Subsequently, the cells were lysed and treated with ultrasound to fragment chromatin ranging from approximately 200 bp to several kilobytes in length. Chromatin fragments were incubated overnight with corresponding antibodies against the target protein and protein G magnetic beads for ChIP. Then, the chromatin fragments were eluted from the antibody/protein G microbeads and de-cross-linked. Finally, the purified DNA was analyzed using qPCR and the primer sets used are presented in **Table S1**.

Xenografted tumor model

Five-week-old male NOD-PrkdcscidIL2rgtm1 (NSIG) mice (Beijing HFKBIOSCIENCE Co., Beijing, China) were subcutaneously injected with MDM1-OE, MDM1-KO HCT8 and RKO cells (2×10^6 in 100 μL PBS). The mice were randomly categorized into vehicle- and chemoradiotherapy-treated groups. Mice in the chemoradiotherapy-treated group received radiotherapy (4 Gy) and intraperitoneal chemotherapy (20 mg/kg 5-FU and 5 mg/kg of oxaliplatin) for 2 weeks, whereas mice in the control group received the same frequency and dose of normal saline injections. Mice treated with RG7388 (10 mg/kg) with or without a combination of chemoradiotherapy treatment were randomly divided.

Bioinformatics analysis

MDM1 expression was analyzed using Gene Expression Profiling Interactive Analysis (GEPIA) and the University of Alabama at the Birmingham CANcer Data Analysis Portal (UALCAN). Next, the prognostic significance of *MDM1* expression in colon cancer was evaluated using the Kaplan–Meier plotter database. The Metascape database (http://metascape.org/) was used for the enrichment analysis.

Statistical analysis

Data were analyzed using GraphPad Prism 7 software. All data were presented as the mean ± SD. A normality test was performed to confirm that each group of samples met the normal distribution and group differences were examined using Student's *t*-test. Survival analysis of DFS time was based on the Kaplan–Meier method and log-rank test with survival outcome variables defining tumor progression or patient death as terminal events. All statistical tests were two-tailed with statistical significance defined as a $P < 0.05$.

Results

MDM1 expression affects the sensitivity of CRC cells to chemoradiotherapy

In two previous studies aimed at identifying biomarkers predicting the sensitivity of CRC cells to chemoradiotherapy[7,20], we conducted gene expression profiling analysis of 81 patients with rectal cancer who underwent and responded differently to preoperative synchronous chemotherapy combined with radical surgery (**Table S2**). This analysis revealed 179 probes representing 132 DEGs between the sensitive and insensitive groups. These DEGs were sorted by *P* value and the function of the top 10 genes was experimentally verified, indicating that *MDM1* expression correlated with the sensitivity of CRC cells to chemoradiotherapy. We also found that *MDM1* expression was lower in non-responders (TRG4+5) and patients with high *MDM1* expression had a better preoperative chemoradiation response and a longer DFS time than patients with low *MDM1* expression (HR = 0.50, 95% CI, 0.27–0.95, $P_{\text{log-rank}} = 0.0337$; **Figure 1A, B**). Therefore, we propose that *MDM1* is a key gene affecting the sensitivity of CRC cells to chemoradiotherapy. Furthermore, a search in the GEPIA database revealed that *MDM1* expression is lower in several tumors, including CRC, than in normal tissues (**Figure 1C, D**). The prognostic value of *MDM1* was evaluated and colon cancer patients expressing high *MDM1* were shown to live longer than patients expressing low *MDM1* (HR = 0.64, 95% CI, 0.52–0.80, $P_{\text{log-rank}} < 0.0001$; **Figure 1E**).

To explore whether MDM1 expression affects the sensitivity of CRC cells to ionizing radiation (IR) and chemotherapeutic treatment, the CRC cell lines (HCT8 and RKO) were engineered into MDM1-KO and MDM1-OE (**Figure 1F, G**). MDM1 silencing decreased the sensitivity to 5-FU and oxaliplatin (**Figure S1A, B**) compared to the control group, whereas MDM1-OE increased chemosensitivity of the cells (**Figure S1C, D**). Extreme limiting dilution analysis showed that MDM1-KO desensitized CRC cells to radiation (**Figure S1E, F**) and MDM1-OE induced IR sensitivity (**Figure S1G, H**). Therefore, we concluded that MDM1 expression affected the sensitivity of CRC cells to radiation and chemotherapy. The cell proliferation and colony-forming abilities were like the control cells when the MDM1-KO and MDM1-OE cells were not subjected to chemoradiation treatments. However, after chemoradiation treatments, the proliferation and colony-forming abilities of MDM1-KO RKO and HCT8 cells were markedly enhanced relative to the control cells (**Figures 2A** and **S2A**) but substantially decreased when MDM1 was overexpressed (**Figures 2B** and **S2B**). Similarly, knockout or overexpression of MDM1 did not alter the growth rate of RKO and HCT8 cells transplanted into mice that did not receive chemoradiation. The growth rates of subcutaneously transplanted tumors accelerated in MDM1-KO cells compared to control cells (**Figures 2C** and **S2C**) in the chemoradiotherapy-treated group, whereas the transplanted tumors exhibited better chemoradiotherapy responses in MDM1-OE cells than control cells (**Figures 2D** and **S2D**).

MDM1 regulates p53 and apoptosis pathways

Currently, only a few studies involving MDM1 and relevant studies on the role of MDM1 in tumor therapy have been published. RNA sequencing was performed to determine MDM1 function. The MDM1-OE group had 542 upregulated and 501 downregulated genes compared to the control group (**Figure 3A**). Kyoto Encyclopedia of Genes and Genomes (KEGG) enrichment analysis of the upregulated genes showed enrichment in small-cell lung cancer, p53 signaling, and apoptosis pathways (**Figure 3B**), while the downregulated genes were accumulated in DNA replication and cell cycle pathways (**Figure 3C**). Gene Set Enrichment Analysis demonstrated

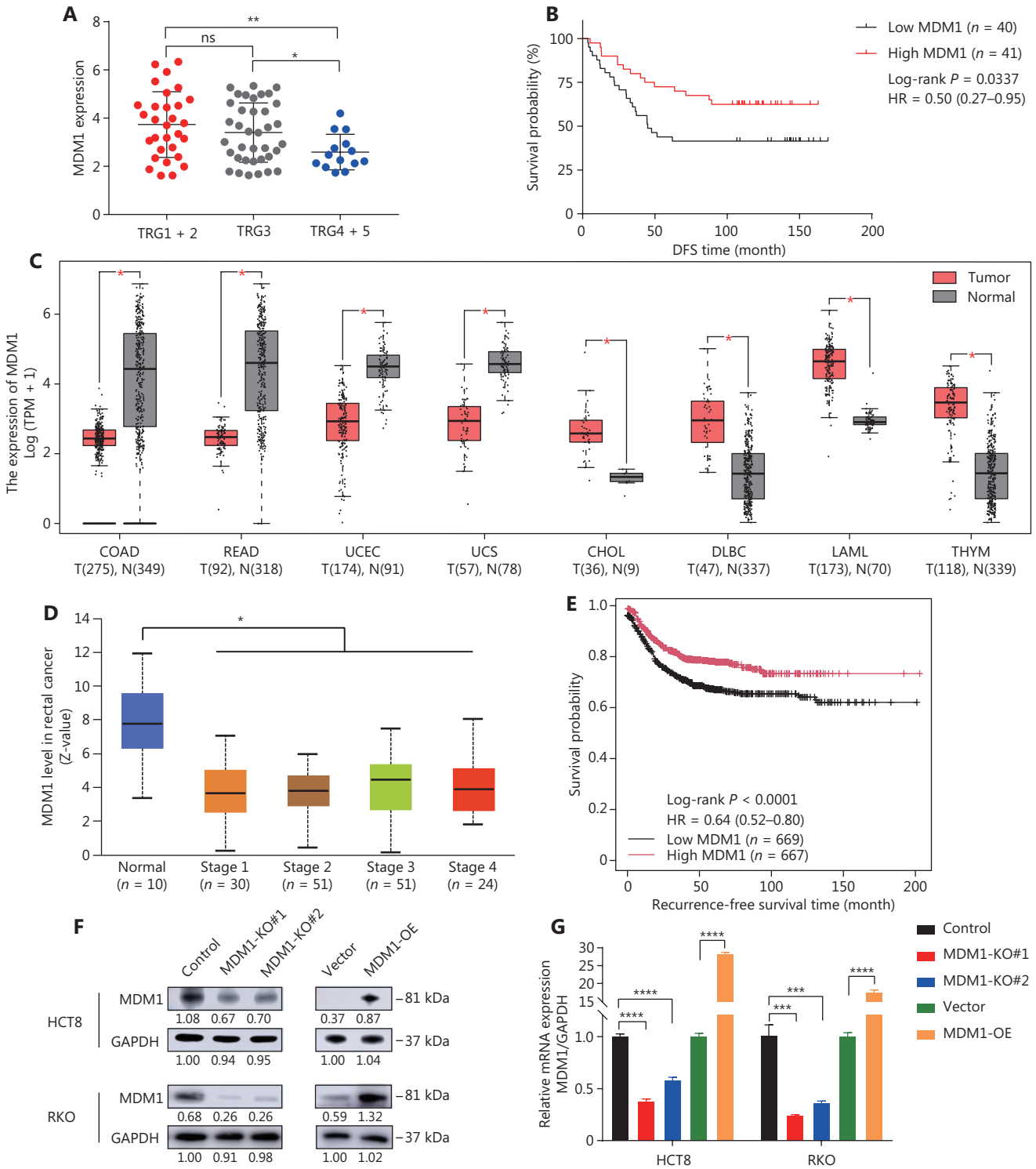


Figure 1 Expression of *MDM1* across cancers and CRC cell lines after silencing or overexpressing MDM1. (A) Expression of *MDM1* among samples of TRG1+2, TRG3, and TRG4+5. Data are shown as the mean ± SD. (B) Kaplan–Meier curves of disease-free survival according to *MDM1* expression in the 81-sample set. Low and high *MDM1* expression groups were distinguished according to the median chip detection values. (C) Expression of *MDM1* across cancers investigated *via* GEPIA. COAD, colon adenocarcinoma; READ, rectum adenocarcinoma; UCEC, uterine corpus endometrial carcinoma; UCS, uterine carcinosarcoma; CHOL, cholangiocarcinoma; DLBC, lymphoid neoplasm diffuse large B-cell lymphoma; LAML, acute myeloid leukemia; THYM, thymoma; T, tumor tissues; N, normal tissues. The numbers in brackets represent the

sample size. (D) Expression of *MDM1* across different stages in TCGA-READ. (E) Kaplan–Meier estimates of survival time by *MDM1* expression in colon cancer (n = 1,336). (F) Expression of MDM1 in MDM1-KO and MDM1-OE HCT8 and RKO cells identified by western blotting. (G) mRNA expression of MDM1 in MDM1-KO and MDM1-OE HCT8 and RKO cells quantified by RT-qPCR. Data are shown as the mean ± SD from three independent experiments (G). *, P < 0.05; **, P < 0.01; ***, P < 0.001; and ****, P < 0.0001 of Student's t-test (A, C, D, G).

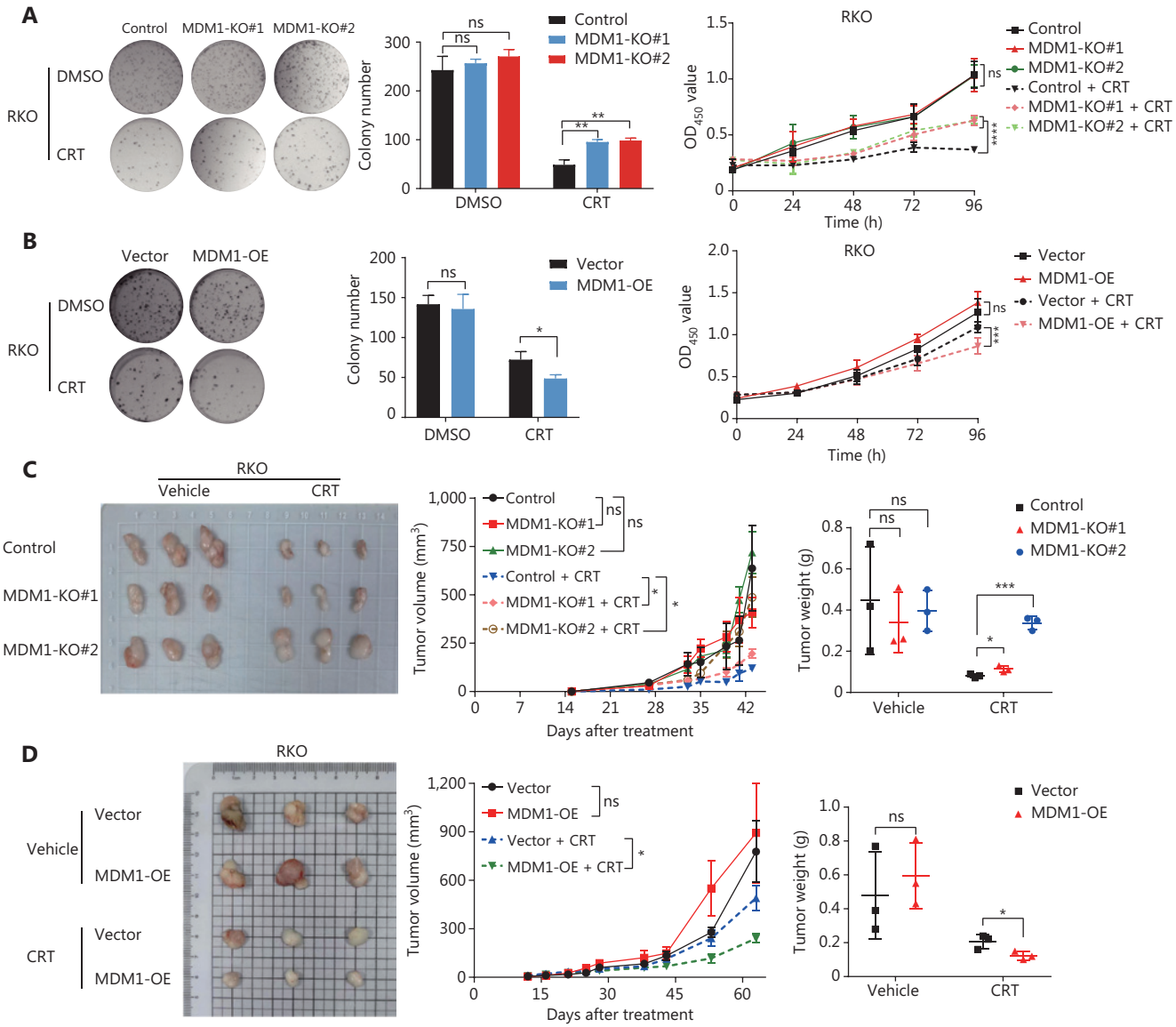


Figure 2 Expression of MDM1 affects the sensitivity of CRC cells to chemoradiation *in vitro* and *in vivo*. (A, B) Colony formation and proliferation curves of the MDM1-KO (A), MDM1-OE (B), and RKO control cells. DMSO, control group treated with DMSO and without radiation (X-ray treatment); CRT, treatment group treated with radiation (2 Gy) and chemotherapy (5 μg/mL of 5-FU and 1 μg/mL of oxaliplatin). Data are shown as the mean ± SD from three independent experiments. (C, D) Images of subcutaneous tumors at the end of the treatment period, proliferation curves, and tumor weights for MDM1-KO (C) and MDM1-OE (D) RKO tumors transplanted in NSIG mice with or without chemoradiotherapy treatment. Data at each time point are the mean ± SEM of tumor volumes from three mice. The right panels represent data (mean ± SEM) of tumor weights from three mice. CRT, treatment group treated with radiotherapy (4 Gy) and chemotherapy (20 mg/kg of 5-FU and 5 mg/kg of oxaliplatin, intraperitoneal administration) for 2 weeks. *, P < 0.05; **, P < 0.01; ***, P < 0.001; ****, P < 0.0001; and ns, not significant of Student's t-test (A–D).

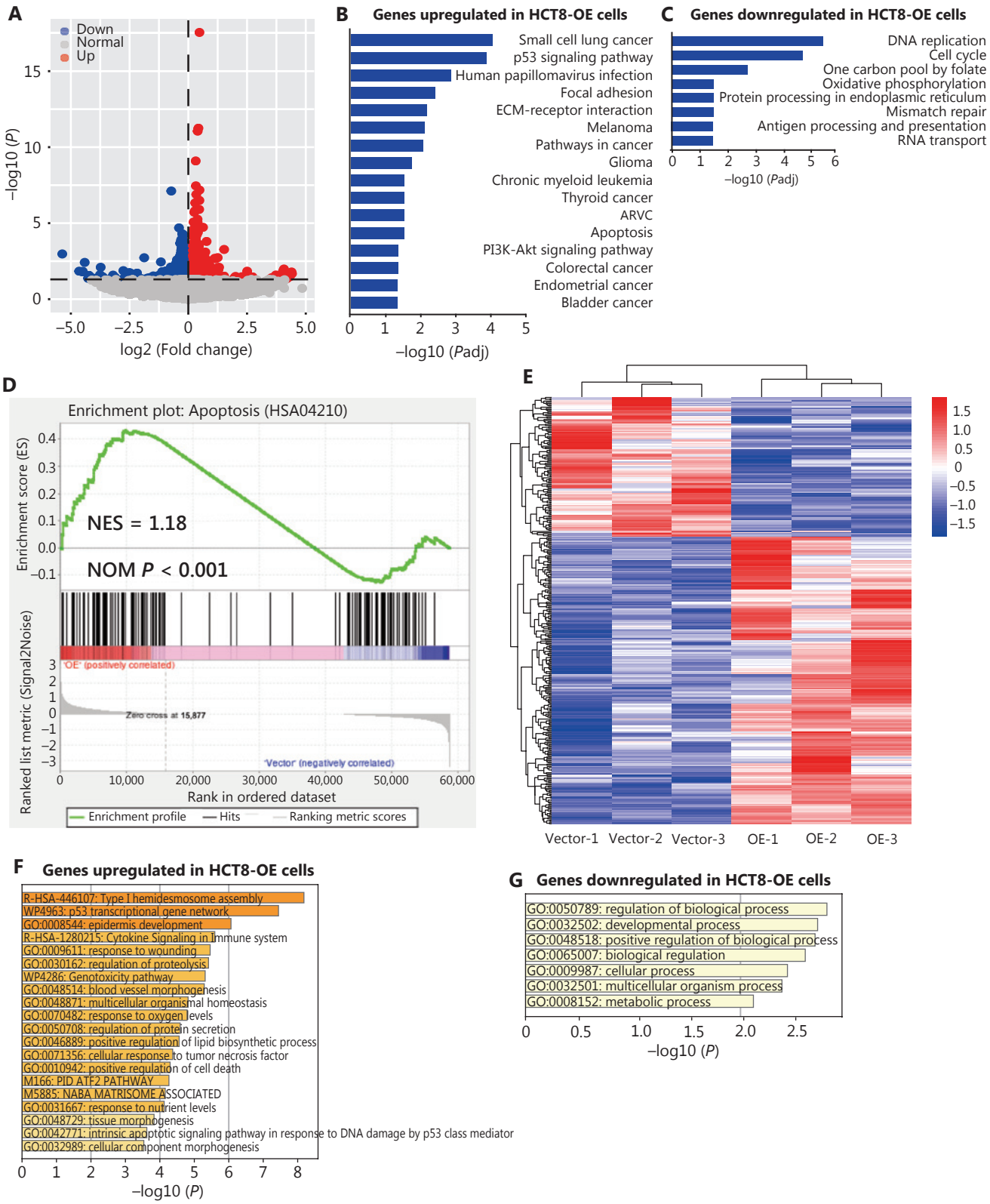


Figure 3 Continued

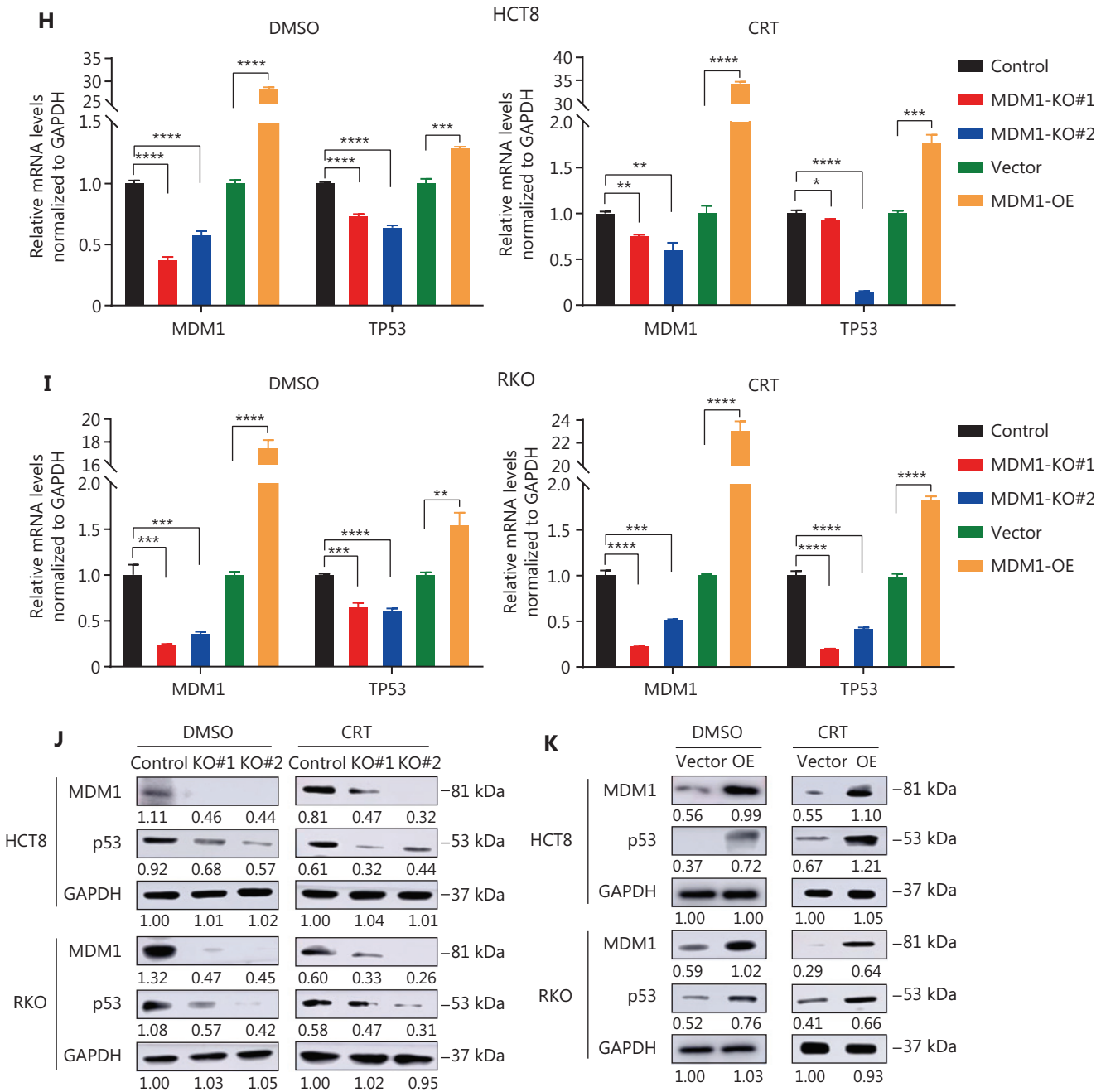


Figure 3 MDM1 regulates p53 signaling and apoptosis pathways. (A) Volcano map showing significantly upregulated (red, fold-change > 1.0) and downregulated (blue, fold-change < 1.0) genes in the MDM1-OE HCT8 cell relative to control cells. (B, C) KEGG pathway enrichment results of 542 upregulated (B, fold-change > 1.0) and 501 downregulated (C, fold-change < 1.0) genes in the MDM1-OE HCT8 cells compared with the control cells. (D) GSEA pathway map of apoptosis ($P < 0.001$, NES = 1.18). (E) Heat map showing DEGs in the MDM1-OE group *vs.* the control group in HCT8 cell lines ($P < 0.05$; fold-change > 1.2 or < 0.8). (F, G) Enrichment analysis of upregulated (F) and downregulated (G) genes in the MDM1-OE HCT8 cells using the public Metascape database ($P < 0.05$; fold-change > 1.2 or < 0.8). (H–K) Expression of MDM1 and p53 in the MDM1-KO and MDM1-OE HCT8 and RKO cell lines identified by RT-qPCR (H, I) and western blotting (J, K) before and after chemoradiation treatment. Data are shown as the mean ± SD from three independent experiments. **, $P < 0.01$; ***, $P < 0.001$; and ****, $P < 0.0001$ of Student's *t*-test (H and I).

that the upregulated genes correlated with autophagy, amino acid metabolism, NF-κB, and apoptosis pathways (**Figure 3D** and **Table S3**), while the downregulated genes were engaged in terpenoid backbone biosynthesis, nitrogen metabolism, and citrate cycle pathways (**Table S4**). When a fold-change of > 1.2 or < 0.8 was evaluated, 236 upregulated and 115 downregulated genes were identified (**Figure 3E**). Enrichment analysis of these DEGs suggested that the upregulated genes were associated with the type I hemidesmosome assembly, p53 signaling pathway, and cell death pathways (**Figure 3F**), while the downregulated genes were mostly involved in biological regulatory processes (**Figure 3G**). In addition, KEGG enrichment analyses of 2,628 upregulated and 3,058 downregulated genes in the MDM1-KO HCT8 cells *vs.* control cells suggested that the downregulated genes were correlated with p53 signaling pathway (**Figure S3A–C**). An enrichment analysis of 157 overlapping genes between the downregulated genes in the MDM1-KO HCT8 cells and upregulated genes in the MDM1-OE HCT8 cells was performed (**Figure S3D**). These genes were related to p53 signaling, apoptosis, and cell death pathways (**Figure S3E**). Proteomic analysis was also performed on the control and MDM1-OE HCT8 cells, confirming 613 differentially expressed proteins (**Figure S3F**). Further analysis revealed 123 significantly altered proteins, including 85 upregulated (fold-change > 1.5) and 37 downregulated proteins (fold-change < 0.6; **Figure S3G**). Enrichment analysis of the 37 downregulated proteins showed that the downregulated proteins were related to negative regulation of the apoptosis pathway (**Figure S3H**).

Considering the mechanisms that may cause tumor resistance, we hypothesized that MDM1 affects the sensitivity of CRC cells to chemoradiotherapy by affecting the p53 signaling and apoptosis pathways. The relationship between MDM1 and p53 expression was subsequently evaluated. RT-qPCR and western blotting verified that before and after chemoradiation treatment, p53 expression dropped in the MDM1-KO cells relative to control cells but increased in the MDM1-OE cells (**Figure 3H–K**).

MDM1 expression regulates CRC cell apoptosis

Flow cytometry proved that apoptosis was considerably repressed in MDM1-KO cells compared to control cells (**Figure 4A**) but was upregulated before and after chemoradiation treatment in the MDM1-OE cells (**Figure 4B**). The impact of MDM1 expression on the apoptotic signaling pathway was verified by western blotting. When not subjected to chemoradiation, cleaved caspase-3, cleaved PARP, and the pro-apoptotic effector (BAX) expression was lower in the MDM1-KO cells *vs.* control cells and the expression difference was more pronounced after chemoradiation treatment (**Figure 4C**). In contrast, cleaved caspase-3, cleaved PARP, and BAX expression was elevated in the MDM1-OE cells before and after chemoradiation treatment (**Figure 4D**). The expression of apoptosis-related genes was examined, including *BAX*, *BAK*, *FAS*, and *GADD45A*, all of which are regulated by p53. The expression of these genes decreased after MDM1-KO (**Figure 4E, F**) but increased after MDM1-OE (**Figure 4G, H**). Therefore, these data suggested that MDM1 affects apoptosis by influencing the level of *TP53* transcription.

MDM1 affects TP53 transcription through its interaction with YBX1

To investigate how MDM1 modulates the level of *TP53* transcription, immunoprecipitation was performed using MDM1 antibodies in the HCT8 cells. Mass spectrometry results showed that the top proteins bound to MDM1 were mostly components of paraspeckles, such as NONO, SFPQ, and paraspeckle protein component 1 (PSPC1), which regulate RNA transcription and splicing (**Figure S4A, B** and **Tables S5–S8**). NONO and SFPQ are the core proteins of paraspeckles. Moreover, YBX1 (also known as YB1) was detected in separate mass spectrometry results of 4 different bands, which has been reported as a transcriptional repressor of p53[21]. Inhibiting YBX1 upregulates p53, resulting in significant apoptosis in a p53-dependent manner. A co-immunoprecipitation assay confirmed MDM1 binding to NONO, SFPQ, and YBX1 in the HCT8 and RKO cell lines (**Figure 5A**). The expression profiling data herein indicated no statistical difference in NONO, SFPQ and YBX1 expression between responders and non-responders to chemoradiotherapy (**Figure S4C–E**). No significant correlation between YBX1 and MDM1 was detected (**Figure S4F**). Therefore, we hypothesized that MDM1 binds to paraspeckles and the p53 transcriptional inhibitor, YBX1, affecting the function of YBX1 and regulating the level of *TP53* transcription to influence cell apoptosis.

First, we verified the interaction between YBX1and the *TP53* promoter region in HCT8 cells by ChIP-qPCR (**Figure S5A**). Western blotting and RT-qPCR analyses showed that *TP53* expression increased after silencing YBX1 (**Figure S5B–D**) and proved that YBX1 inhibits *TP53* transcription. Furthermore, mRNA expression of apoptosis-related genes downstream

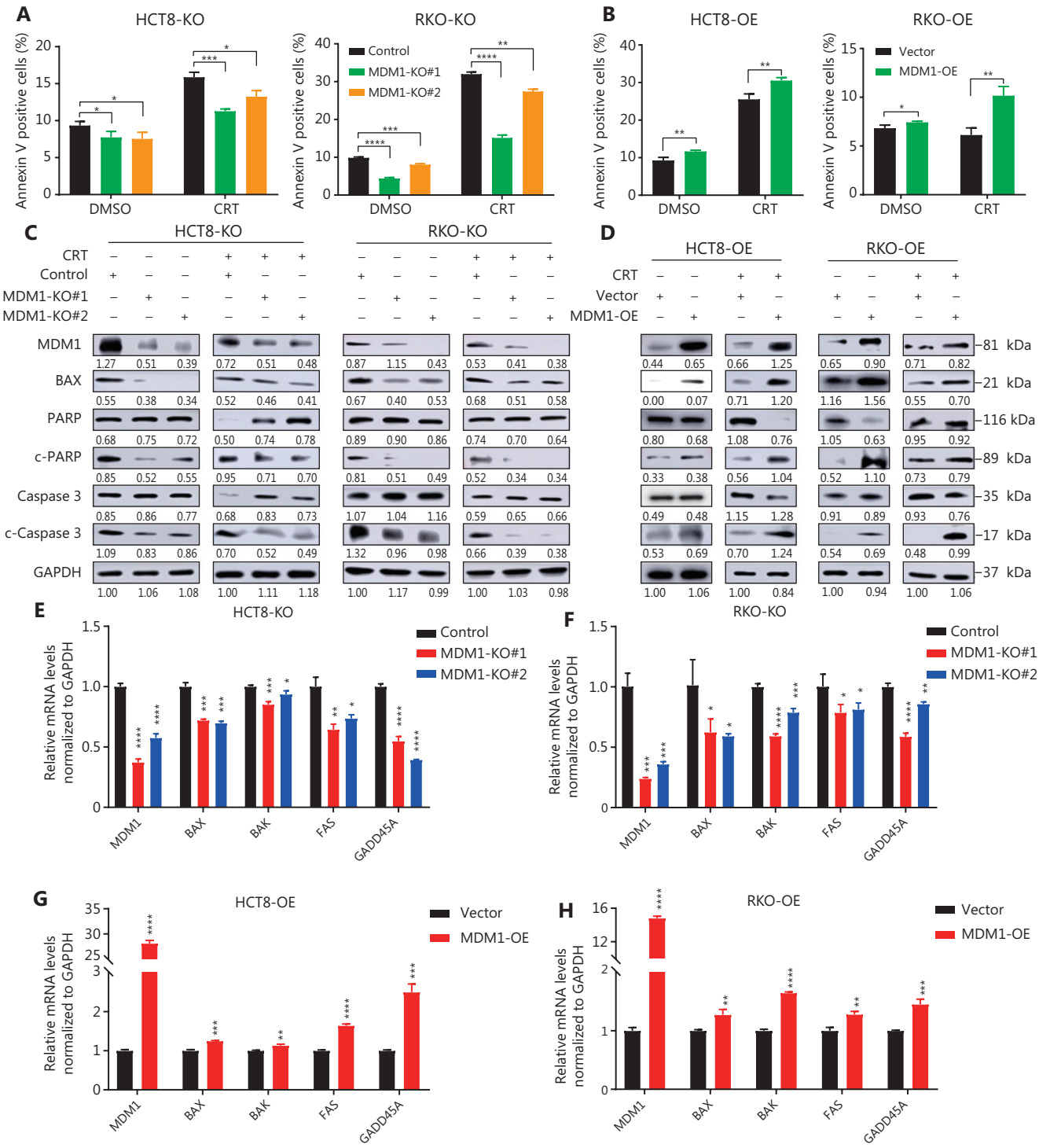


Figure 4 MDM1 expression regulates CRC cell apoptosis. (A) Proportion of apoptotic MDM1-KO HCT8 and RKO cells in chemoradiotherapy-treated and control groups. (B) Proportion of apoptotic MDM1-OE HCT8 and RKO cells in chemoradiotherapy-treated and control groups. (C) Western blots of MDM1 and several apoptosis-related protein levels in chemoradiotherapy-treated and control groups of MDM1-KO HCT8 and RKO cells. (D) Western blots of MDM1 and several apoptosis-related proteins in chemoradiotherapy-treated and control groups of MDM1-OE HCT8 and RKO cells. (E, F) mRNA expression of MDM1 and apoptosis-related genes detected by RT-qPCR in MDM1-KO HCT8 (E) and RKO (F) cells. (G, H) mRNA expression of MDM1 and apoptosis-related genes detected by RT-qPCR in MDM1-OE HCT8 (G) and RKO (H) cells. Data are shown as the mean ± SD from three independent experiments. *, $P < 0.05$; **, $P < 0.01$; ***, $P < 0.001$; and ****, $P < 0.0001$ of Student's *t*-test (A, B, E–H).

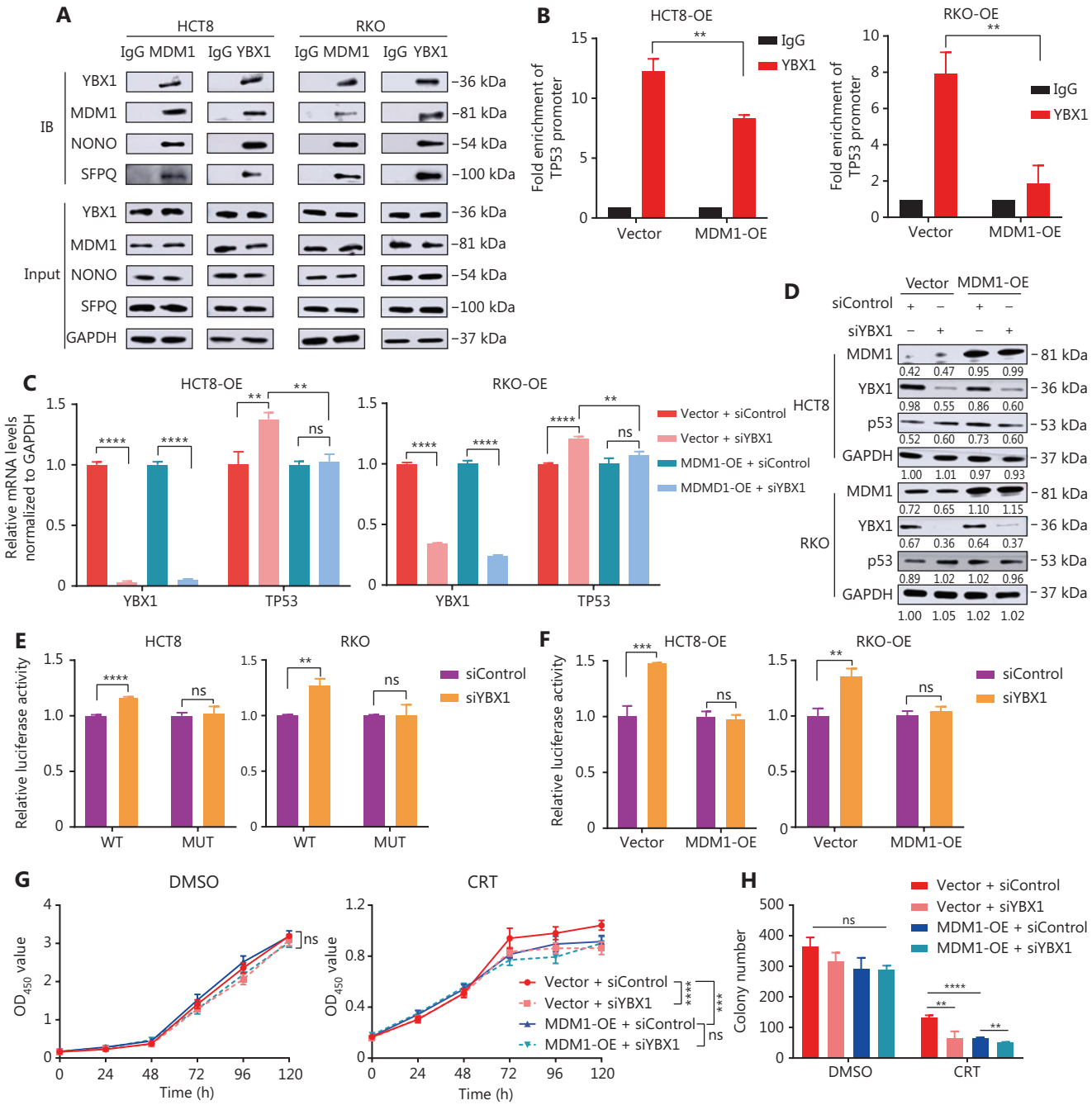


Figure 5 MDM1 affects *TP53* transcription through interaction with YBX1. (A) Immunoprecipitation was performed with antibodies to MDM1 and YBX1 in HCT8 and RKO cell lines. MDM1, YBX1, NONO, and SFPQ antibodies were used for the western blotting assay. (B) ChIP-qPCR results showing the enrichment of the *TP53* promoter in the MDM1-OE group *vs.* the control group in HCT8 and RKO cell lines. (C, D) mRNA (C) and protein (D) expression of YBX1 and *TP53* measured by real-time quantitative PCR and western blotting assays in MDM1-OE HCT8 and RKO cells with and without YBX1 silencing by siRNA. (E) Luciferase activity of transfection of a plasmid containing wild-type (WT) or mutant (MUT) *TP53* promoter region in HCT8 and RKO cell lines with and without YBX1 silencing by siRNA. (F) Luciferase activity of transfection of a plasmid containing wild-type *TP53* promoter region in MDM1-OE HCT8 and RKO cells with and without YBX1 silencing by siRNA. (G, H) Proliferation curves (G) and colony formation assay (H) of knocking down YBX1 in the MDM1-OE HCT8 and control cells. Data are shown as the mean ± SD from three independent experiments. **, $P < 0.01$; ***, $P < 0.001$, ****, $P < 0.0001$; and ns, not significant of Student's *t*-test (B, C, E–H).

of p53 increased after silencing YBX1 (**Figure S5C–E**). Interestingly, after MDM1-OE the binding of YBX1 to the *TP53* promoter was impaired *vs.* control (**Figure 5B**). Knockdown of YBX1 in MDM1-OE cells did not increase *TP53* expression compared to control cells (**Figure 5C, D**) and the same was noted in *TP53*-mutated HT29 cells (**Figure S5F**). Reporter gene vectors containing the wild-type and mutated *TP53* promoter regions were constructed. Dual-luciferase reporter assays indicated that transfection vectors containing wild-type, but not mutated, *TP53* promoter region increased luciferase activity (**Figures 5E** and **S5G**). When vectors with wild-type *TP53* promoter were transfected into the MDM1-OE and control cells, YBX1 knockdown in MDM1-OE cells failed to increase luciferase activity compared to control cells (**Figures 5F** and **S5H**), demonstrating that MDM1 attenuates the transcriptional inhibition of *TP53* by YBX1. To confirm whether MDM1 affects cell sensitivity to chemoradiotherapy by interacting with YBX1, YBX1 in MDM1-OE and control cells was knocked down. Silencing YBX1 did not affect cell proliferation and colony-forming abilities in vector or MDM1-OE cells in the absence of chemoradiation treatment. After chemoradiation, silencing YBX1 decreased cell proliferation and colony formation abilities in control cells but did not increase cell sensitivity to chemoradiation in MDM1-OE cells (**Figures 5G, H** and **S6A–D**).

Inducing cell apoptosis restores the sensitivity of MDM1-KO cells to chemoradiation

Collectively, cells with high MDM1 expression were sensitive to chemoradiotherapy by influencing the p53-directed apoptotic pathways, whereas cells with low MDM1 expression were resistant to chemoradiotherapy. We speculated that the sensitivity of cells with low MDM1 expression could be restored by inducing apoptosis. Therefore, the dual BCL-2 and BCL-XL inhibitor, navitoclax (ABT-263), the second mitochondrial-derived activator of caspases (SMAC) mimetic, birinapant (TL32711), and the MDM2 inhibitor, idasanutlin (RG7388), were tested. Flow cytometry showed that these three drugs induced apoptosis in MDM1-KO cells in combination with chemoradiation (**Figure 6A, B**). Cloning showed that these three drugs restored the sensitivity of MDM1-KO cells to chemoradiation treatment (1.0 μM RG7388; **Figures 6C, D** and **S7A, B**). Considering that MDM1 affects apoptosis by influencing the transcription level of *TP53*, RG7388 was selected for further *in vivo* experiments. When RG7388 (10 mg/kg) was used alone, the tumor growth rates did not significantly differ between MDM1-KO and control RKO cells. However, the MDM1-KO group was more sensitive to the combination of RG7388 and chemoradiation treatment (**Figure 6E**).

Therefore, targeting the apoptotic pathway is a feasible method for restoring the sensitivity of cells with low MDM1 expression to chemoradiotherapy treatment. Graphical abstract showed that the level of MDM1 expression influences the sensitivity of CRC cells to chemoradiotherapy by regulating p53 signaling and apoptosis pathways (**Figure 7**). The sensitivity of CRC cells to chemoradiotherapy increased after MDM1-OE and decreased after MDM1-KO. MDM1-OE can eliminate the binding of YBX1 to the *TP53* promoter, upregulate *TP53* transcription, and render CRC cells more sensitive to chemoradiation. MDM1-KO downregulates *TP53* expression and cell apoptosis, leading to treatment resistance. For CRC cells with low levels of MDM1 expression, the combination of apoptosis-inducing inhibitors and chemoradiotherapy could restore the sensitivity of MDM1-KO cells to cancer therapy.

Discussion

In a previous study screening for differential transcripts of genes related to chemoradiotherapy sensitivity, a correlation between MDM1 expression and sensitivity to chemoradiotherapy in patients with CRC was discovered. Through gene expression profiling analysis of 44 CRC samples with preoperative concurrent chemoradiotherapy, 132 DEGs among patients with different treatment responses were identified with *MDM1* ranking 10th. After knocking down the top 10 DEGs in CRC cell lines, the cells were treated with chemoradiotherapy and *MDM1* ranked 3rd according to *P* values in the colony formation assay. Because studies on the *ZNF37A* (the top one gene) mechanisms of action have already been completed, ZNF37A downregulation promotes TNFRSF6B expression, inhibits apoptosis, and leads to therapeutic resistance to concurrent chemoradiotherapy in patients with rectal cancer[7]; the current study focused on *MDM1*.

Further data analysis indicated that patients with high *MDM1* expression responded better to chemoradiation and had an extended DFS time than patients with low *MDM1* expression. Therefore, *MDM1* expression was verified to affect the sensitivity of CRC cells to chemoradiotherapy treatment. RNA sequencing and further experiments revealed a correlation between MDM1 expression and the p53 signaling and

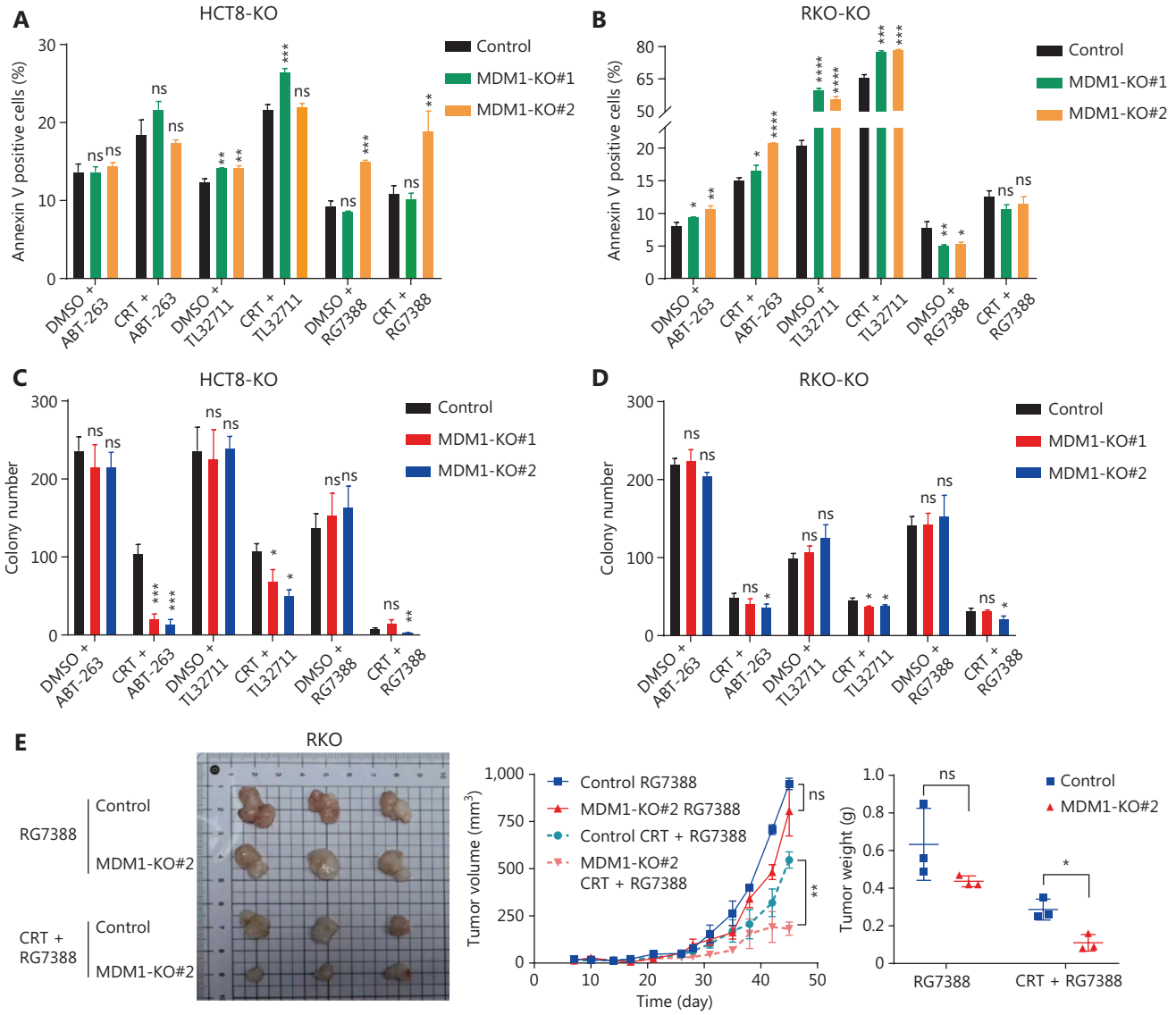


Figure 6 Inducing cell apoptosis restores the sensitivity of MDM1-KO cells to chemoradiotherapy treatment. (A, B) Proportions of apoptotic cells in the MDM1-KO HCT8 (A) and RKO (B) cells after treatment with inhibitors targeting apoptosis (ABT-263, TL32711, and RG7388) with or without the combination of chemoradiation treatment. (C, D) Colony number of the MDM1-KO HCT8 (C) and RKO (D) cells after treatment with inhibitors targeting apoptosis (ABT-263, TL32711, and RG7388) with or without the combination of chemoradiation treatment. (E) Images of subcutaneous tumors at the end of the treatment period, proliferation curves, and tumor weights for the MDM1-KO RKO tumors transplanted into NSIG mice treated with RG7388 with or without chemoradiation treatment. Data at each time point are shown as the mean ± SEM of tumor volumes from three mice. The right panels represent data (mean ± SEM) of tumor weights from three mice. Data are shown as the mean ± SD from three independent experiments (A–D). *, $P < 0.05$; **, $P < 0.01$; ***, $P < 0.001$; ****, $P < 0.0001$; and ns, not significant of Student's *t*-test (A–E).

apoptosis pathways. MDM1 was shown to bind to NONO, SFPQ, and YBX1. MDM1-OE reduced binding of YBX1 to the *TP53* promoter, weakened the transcriptional inhibition of YBX1 on *TP53*, and sensitized CRC cells to chemoradiation. For CRC cells with low MDM1 expression that were resistant to chemoradiotherapy, three drugs targeting the apoptotic pathway were tested, particularly MDM2 inhibitors targeting p53. The results indicated that inducing apoptosis restored the sensitivity of MDM1-KO cells to chemoradiotherapy. This finding provides a potential treatment option to restore

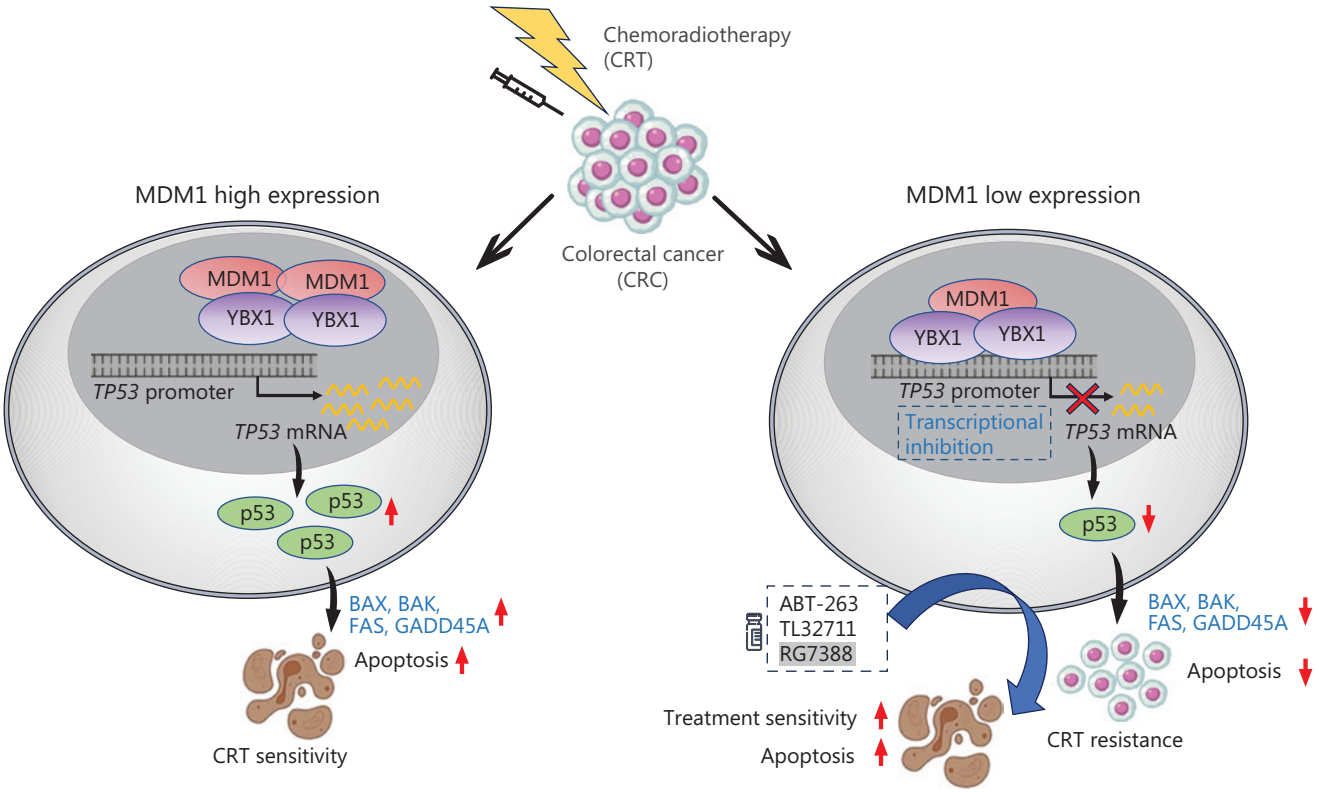


Figure 7 Working model: MDM1 regulates therapeutic sensitivity to chemoradiotherapy in colorectal cancer. The sensitivity of CRC cells to chemoradiotherapy increased after MDM1-OE and decreased after MDM1-KO. MDM1-OE eliminate binding of YBX1 and *TP53* promoter, upregulate *TP53* transcription, and make CRC cells more sensitive to chemoradiation. MDM1-KO downregulate *TP53* expression and cell apoptosis, leading to treatment resistance. Combination of inhibitors inducing apoptosis and chemoradiotherapy restored the sensitivity of MDM1-KO cells to cancer therapy because CRC cells have low MDM1 expression.

sensitivity to chemoradiotherapy in patients with low MDM1 expression (**Figure 7**).

The current study confirmed the interactions of MDM1 with YBX1, NONO, and SFPQ. YBX1 is responsible for regulating multiple biological activities, including cell propagation, differentiation, senescence, apoptosis, and tumor development[22,23]. *YBX1* encodes proteins that bind DNA and RNA, participating in processes, such as translation inhibition, RNA stabilization, mRNA splicing, DNA repair, and transcriptional modulation[23-26]. YBX1 predominantly acts as an RNA-binding protein that specifically recognizes and binds to 5-methylcytosine-modified mRNA transcripts and promotes mRNA stabilization[27,28]. YBX1 also acts as a transcription factor binding to a promoter containing Y-box (5′-CTGATTGGCCAA-3′), such as *TP53*, negatively regulating *TP53* expression and p53-induced cell death[21,29-31]. The current study demonstrated that MDM1 regulates *TP53* transcription through MDM1 interaction with YBX1, influencing the CRC sensitivity to chemoradiation. Notably, although MDM1 affects p53 expression, MDM1 did not show tumorigenicity[15], which may be the result of crosstalk between distinct biochemical processes[32,33].

NONO and SFPQ are core proteins involved in the formation of paraspeckles, which regulate gene expression by altering the distribution of paraspeckle proteins, RNA retention, and interactions with microRNAs[34,35]. NONO and SFPQ share a common domain consisting of two RNA recognition motifs, belonging to the *Drosophila melanogaster* behavior, human splicing (DBHS) protein family and exerting multiple regulatory effects[36]. NONO, a multifunctional nuclear protein, regulates gene expression through RNA splicing, transcriptional activation, and termination and participates in biological activities, such as cell propagation, apoptosis, migration, and DNA damage repair[37]. Studies have reported that NONO exerts dual effects on apoptosis, either promoting or inhibiting apoptosis[38,39]. SPFQ activates several BCL-2

family pro-apoptosis genes associated with chemotherapy sensitivity[40]. In the current study the combination of MDM1 with YBX1, NONO, and SFPQ was proven through immunoprecipitation experiments. However, the specific roles of NONO and SFPQ remain unclear. Given the diverse functions of paraspeckles, MDM1, as a potential new paraspeckle component, may affect many other genes and molecules, warranting further research.

Interestingly, the current study demonstrated that MDM1 and ZNF37A affect chemoradiotherapy sensitivity by influencing cell apoptosis, which is consistent with the recognized perception that resistance to apoptosis leads to poor therapeutic outcomes in patients with cancer[41]. Effective killing of cancer cells through programmed cell death or apoptosis has always been a major goal of clinical cancer therapy. The equilibrium between pro- and anti-apoptotic BCL-2 family members controls cytochrome c release from mitochondria and in turn activates caspases, which are negatively regulated by the inhibitor of apoptosis protein (IAP) family[42-44]. BH3 mimetics are small-molecule inhibitors targeting pro-survival BCL-2 family members, inducing apoptosis downstream of p53. Venetoclax (ABT-199), a BH3 mimetic targeting BCL-2, has been approved by regulatory authorities worldwide for treating chronic lymphocytic and acute myeloid leukemia and second-generation navitoclax (ABT-263) has been developed and tested[45,46]. Inhibitor of apoptosis proteins (IAPs) promote cell survival by preventing caspase activation[47] and IAP inhibitors, commonly referred to as SMAC mimetics, such as birinapant (TL32711) and LCL161, can be safely combined with various chemotherapeutics[48]. P53 modulates the expression of apoptosis-associated target genes and promotes apoptosis[32]. Specifically, the MDM2 inhibitor, nutlins, induces p53 activation in wild-type p53 cancer cells and a third-generation nutlin derivative, idasanutlin (RG7388), is undergoing clinical trials[49]. The current study showed that ABT-263, TL32711, and RG7388 induce apoptosis and weaken resistance of MDM1-KO cells to chemoradiation treatment. *In vivo* studies demonstrated that the MDM1-KO cells were highly sensitive to treatment after combining RG7388 with chemoradiation. This provides a possible treatment strategy for increasing the sensitivity of CRC cells to chemoradiotherapy. Although numerous studies on drugs targeting p53 are ongoing, much remains to be explored before the transition of p53-targeted drugs to the clinic and the current difficulty in developing p53-targeted drugs limits this study[50,51].

Conclusions

The findings herein indicate that MDM1 is a prospective predictive marker for CRC sensitivity to chemoradiotherapy, thereby providing guidance for the development of individualized treatment regimens.

Acknowledgments

We would like to express our sincere gratitude to the patients and clinicians who participated in this study. We extend special thanks to Kaitai Zhang and Xuebin Di for providing genome-wide expression profiling data services.

Grant support

This work was supported by grants from the National Natural Science Foundation (Grant No. 81972859 to W.T.), Beijing Municipal Science & Technology Commission Grant (Grant No. D0905001040531 to D.L.), and State Key Laboratory of Molecular Oncology Grant (Grant No. SKLMO-KF2023-03 to D.L.).

Conflict of interest statement

No potential conflicts of interest are disclosed.

Author contributions

Designed and conducted most experiments: Ningxin Ren, Hongxia Chen, and Ying Huang.
Collected the data: Jing Jin, Shuangmei Zou, Yexiong Li.
Bioinformatics and statistical analysis: Shaosen Zhang, Ruoqing Yan, Mengjie Li, Linlin Zheng.
Wrote the paper: Ningxin Ren, Hongxia Chen, Wen Tan, and Dongxin Lin.

Data availability statement

The public databases used in this study include Gene Expression Profiling Interactive Analysis (GEPIA [http://gepia.cancer-pku.cn/]), the University of Alabama at the Birmingham CANcer Data Analysis Portal (UALCAN [http://ualcan.path.uab.edu/index.html]), Kaplan–Meier plotter database (https://kmplot.com/analysis/), and Metascape database

(http://metascape.org/). The genome-wide expression profiling data of 81 patients with rectal cancer who received neoadjuvant chemoradiotherapy were submitted to the National Genomic Data Center database (https://ngdc.cncb.ac.cn/gsub/ [project ID: PRJCA027384]). Other data will be obtained from the first author, Ningxin Ren, upon reasonable request.

References

1. Sauer R, Liersch T, Merkel S, Fietkau R, Hohenberger W, Hess C, et al. Preoperative versus postoperative chemoradiotherapy for locally advanced rectal cancer: results of the German CAO/ARO/AIO-94 randomized phase III trial after a median follow-up of 11 years. J Clin Oncol. 2012; 30: 1926-33.
2. Sun XX, Dai MS, Lu H. 5-Fluorouracil activation of p53 involves an MDM2-ribosomal protein interaction. J Biol Chem. 2007; 282: 8052-59.
3. Ma J, Zhu J, Li J, Liu J, Kang X, Yu J. Enhanced E6AP-mediated ubiquitination of ENO1 via LINC00663 contributes to radiosensitivity of breast cancer by regulating mitochondrial homeostasis. Cancer Lett. 2023; 560: 216118.
4. Garcia-Barros M, Paris F, Cordon-Cardo C, Lyden D, Rafii S, Haimovitz-Friedman A, et al. Tumor response to radiotherapy regulated by endothelial cell apoptosis. Science. 2003; 300: 1155-9.
5. Gottesman MM. Mechanisms of cancer drug resistance. Annu Rev Med. 2002; 53: 615-27.
6. Machado Carvalho JV, Dutoit V, Corrò C, Koessler T. Promises and challenges of predictive blood biomarkers for locally advanced rectal cancer treated with neoadjuvant chemoradiotherapy. Cells. 2023; 12: 413.
7. Huang Y, Jin J, Ren N, Chen H, Qiao Y, Zou S, et al. ZNF37A downregulation promotes TNFRSF6B expression and leads to therapeutic resistance to concurrent chemoradiotherapy in rectal cancer patients. Transl Oncol. 2025; 51: 102203.
8. Kastan MB, Canman CE, Leonard CJ. P53, cell cycle control and apoptosis: implications for cancer. Cancer Metastasis Rev. 1995; 14: 3-15.
9. Williams AB, Schumacher B. p53 in the DNA-damage-repair process. Cold Spring Harb Perspect Med. 2016; 6: a026070.
10. Fridman JS, Lowe SW. Control of apoptosis by p53. Oncogene. 2003; 22: 9030-40.
11. Daujat S, Neel H, Piette J. MDM2: life without p53. Trends Genet. 2001; 17: 459-64.
12. Hou H, Sun D, Zhang X. The role of *MDM2* amplification and overexpression in therapeutic resistance of malignant tumors. Cancer Cell Int. 2019; 19: 216.
13. Kondo S, Barnett GH, Hara H, Morimura T, Takeuchi J. MDM2 protein confers the resistance of a human glioblastoma cell line to cisplatin-induced apoptosis. Oncogene. 1995; 10: 2001-6.
14. Hayashi S, Ozaki T, Yoshida K, Hosoda M, Todo S, Akiyama S, et al. p73 and MDM2 confer the resistance of epidermoid carcinoma to cisplatin by blocking p53. Biochem Biophys Res Commun. 2006; 347: 60-6.
15. Fakharzadeh SS, Trusko SP, George DL. Tumorigenic potential associated with enhanced expression of a gene that is amplified in a mouse tumor cell line. EMBO J. 1991; 10: 1565-9.
16. Hoh RA, Stowe TR, Turk E, Stearns T. Transcriptional program of ciliated epithelial cells reveals new cilium and centrosome components and links to human disease. PLoS One. 2012; 7: e52166.
17. Van de Mark D, Kong D, Loncarek J, Stearns T. MDM1 is a microtubule-binding protein that negatively regulates centriole duplication. Mol Biol Cell. 2015; 26: 3788-802.
18. Hariri H, Speer N, Bowerman J, Rogers S, Fu G, Reetz E, et al. MDM1 maintains endoplasmic reticulum homeostasis by spatially regulating lipid droplet biogenesis. J Cell Biol. 2019; 218: 1319-34.
19. Son Y, Kim SJ, Kim HY, Lee J, Kim JR. MDM1 ablation results in retinal degeneration by specific intraflagellar transport defects of photoreceptor cells. Cell Death Dis. 2022; 13: 833.
20. Yang J, Lin Y, Huang Y, Jin J, Zou S, Zhang X, et al. Genome landscapes of rectal cancer before and after preoperative chemoradiotherapy. Theranostics. 2019; 9: 6856-66.
21. Lasham A, Moloney S, Hale T, Homer C, Zhang YF, Murison JG, et al. The Y-box-binding protein, YB1, is a potential negative regulator of the p53 tumor suppressor. J Biol Chem. 2003; 278: 35516-23.
22. Feng M, Xie X, Han G, Zhang T, Li Y, Li Y, et al. YBX1 is required for maintaining myeloid leukemia cell survival by regulating BCL2 stability in an m6A-dependent manner. Blood. 2021; 138: 71-85.
23. Xiao Y, Cai GP, Feng X, Li YJ, Guo WH, Guo Q, et al. Splicing factor YBX1 regulates bone marrow stromal cell fate during aging. EMBO J. 2023; 42: e111762.
24. Gaudreault I, Guay D, Lebel M. YB-1 promotes strand separation in vitro of duplex DNA containing either mispaired bases or cisplatin modifications, exhibits endonucleolytic activities and binds several DNA repair proteins. Nucleic Acids Res. 2004; 32: 316-27.
25. Chen CY, Gherzi R, Andersen JS, Gaietta G, Jürchott K, Royer HD, et al. Nucleolin and YB-1 are required for JNK-mediated interleukin-2 mRNA stabilization during T-cell activation. Genes Dev. 2000; 14: 1236-48.
26. Kwon E, Todorova K, Wang J, Horos R, Lee KK, Neel VA, et al. The RNA-binding protein YBX1 regulates epidermal progenitors at a posttranscriptional level. Nat Commun. 2018; 9: 1734.
27. Ray D, Kazan H, Chan ET, Peña Castillo L, Chaudhry S, Talukder S, et al. Rapid and systematic analysis of the RNA recognition specificities of RNA-binding proteins. Nat Biotechnol. 2009; 27: 667-70.
28. Chen X, Li A, Sun BF, Yang Y, Han YN, Yuan X, et al. 5-Methylcytosine promotes pathogenesis of bladder cancer through stabilizing mRNAs. Nat Cell Biol. 2019; 21: 978-90.
29. Chattopadhyay R, Das S, Maiti AK, Boldogh I, Xie J, Hazra TK, et al. Regulatory role of human AP-endonuclease (APE1/Ref-1) in YB-1-mediated activation of the multidrug resistance gene MDR1. Mol Cell Biol. 2008; 28: 7066-80.
30. Li B, Li F, Gu T, Guo Y, Shen B, Xu X, et al. Specific knockdown of Y-box binding protein 1 in hepatic progenitor cells inhibits

proliferation and alleviates liver fibrosis. Eur J Pharmacol. 2022; 921: 174866.
31. Homer C, Knight DA, Hananeia L, Sheard P, Risk J, Lasham A, et al. Y-box factor YB1 controls p53 apoptotic function. Oncogene. 2005; 24: 8314-25.
32. Kastenhuber ER, Lowe SW. Putting p53 in context. Cell. 2017; 170: 1062-78.
33. Speidel D. Transcription-independent p53 apoptosis: an alternative route to death. Trends Cell Biol. 2010; 20: 14-24.
34. Fox AH, Lam YW, Leung AK, Lyon CE, Andersen J, Mann M, et al. Paraspeckles: a novel nuclear domain. Curr Biol. 2002; 12: 13-25.
35. Yamazaki T, Souquere S, Chujo T, Kobelke S, Chong YS, Fox AH, et al. Functional domains of NEAT1 architectural lncRNA induce paraspeckle assembly through phase separation. Mol Cell. 2018; 70: 1038-53.e7.
36. Bond CS, Fox AH. Paraspeckles: nuclear bodies built on long noncoding RNA. J Cell Biol. 2009; 186: 637-44.
37. Feng P, Li L, Deng T, Liu Y, Ling N, Qiu S, et al. NONO and tumorigenesis: more than splicing. J Cell Mol Med. 2020; 24: 4368-76.
38. Cheng R, Zhu S, Guo S, Min L, Xing J, Guo Q, et al. Downregulation of NONO induces apoptosis, suppressing growth and invasion in esophageal squamous cell carcinoma. Oncol Rep. 2018; 39: 2575-83.
39. King HA, Cobbold LC, Pichon X, Pöyry T, Wilson LA, Booden H, et al. Remodelling of a polypyrimidine tract-binding protein complex during apoptosis activates cellular IRESs. Cell Death Differ. 2014; 21: 161-71.
40. Zeng C, Liu S, Lu S, Yu X, Lai J, Wu Y, et al. The c-Myc-regulated lncRNA NEAT1 and paraspeckles modulate imatinib-induced apoptosis in CML cells. Mol Cancer. 2018; 17: 130.
41. Mohammad RM, Muqbil I, Lowe L, Yedjou C, Hsu HY, Lin LT, et al. Broad targeting of resistance to apoptosis in cancer. Semin Cancer Biol. 2015; 35: S78-S103.
42. Martinou JC, Youle RJ. Mitochondria in apoptosis: Bcl-2 family members and mitochondrial dynamics. Dev Cell. 2011; 21: 92-101.
43. Ledgerwood EC, Morison IM. Targeting the apoptosome for cancer therapy. Clin Cancer Res. 2009; 15: 420-4.
44. Silke J, Meier P. Inhibitor of apoptosis (IAP) proteins-modulators of cell death and inflammation. Cold Spring Harb Perspect Biol. 2013; 5: a008730.
45. Diepstraten ST, Anderson MA, Czabotar PE, Lessene G, Strasser A, Kelly GL. The manipulation of apoptosis for cancer therapy using BH3-mimetic drugs. Nat Rev Cancer. 2022; 22: 45-64.
46. Carneiro BA, El-Deiry WS. Targeting apoptosis in cancer therapy. Nat Rev Clin Oncol. 2020; 17: 395-417.
47. Fulda S, Vucic D. Targeting IAP proteins for therapeutic intervention in cancer. Nat Rev Drug Discov. 2012; 11: 109-24.
48. Fulda S. Promises and challenges of Smac mimetics as cancer therapeutics. Clin Cancer Res. 2015; 21: 5030-6.
49. Liu Y, Su Z, Tavana O, Gu W. Understanding the complexity of p53 in a new era of tumor suppression. Cancer Cell. 2024; 42: 946-67.
50. Song H, Xiao S, Wu J, Lu M. Drugging p53: barriers, criteria, and prospects. Cancer Discov. 2024; 14: 2055-60.
51. Wang L, Wang N, Zhang W, Cheng X, Yan Z, Shao G, et al. Therapeutic peptides: current applications and future directions. Signal Transduct Target Ther. 2022; 7: 48.

Cite this article as: Ren N, Chen H, Huang Y, Jin J, Zhang S, Yan R, et al. MDM1 overexpression promotes p53 expression and cell apoptosis to enhance therapeutic sensitivity to chemoradiotherapy in patients with colorectal cancer. Cancer Biol Med. 2025; 22: 266-283. doi: 10.20892/j.issn.2095-3941.2024.0540